HHS Public Access

Author manuscript

Nat Chem. Author manuscript; available in PMC 2014 May 01.

Published in final edited form as:

Nat Chem. 2013 November ; 5(11): 958–963. doi:10.1038/nchem.1765.

Layer-by-layer Cell Membrane Assembly

Sandro Matosevic and **Brian M. Paegel***

Department of Chemistry, The Scripps Research Institute, 130 Scripps Way, Jupiter, FL 33458

Abstract

Eukaryotic subcellular membrane systems, such as the nuclear envelope or endoplasmic reticulum, present a rich array of architecturally and compositionally complex supramolecular targets that are yet inaccessible. Here we describe layer-by-layer phospholipid membrane assembly on microfluidic droplets, a route to structures with defined compositional asymmetry and lamellarity. Starting with phospholipid-stabilized water-in-oil droplets trapped in a static droplet array, lipid monolayer deposition proceeds as oil/water phase boundaries pass over the droplets. Unilamellar vesicles assembled layer-by-layer support functional insertion of both purified and *in situ* expressed membrane proteins. Synthesis and chemical probing of asymmetric unilamellar and double bilayer vesicles demonstrate the programmability of both membrane lamellarity and lipid leaflet composition during assembly. The immobilized vesicle arrays are a pragmatic experimental platform for biophysical studies of membranes and their associated proteins, particularly complexes that assemble and function in multilamellar contexts *in vivo*.

Phospholipid membranes are complex supramolecular assemblies involved in every aspect of biological function. They drive Darwinian evolution by coencapsulating the cellular metabolism and genetics, and they are universally the means by which Eukarya spatially organize their diverse subcellular metabolic processes. These structures have many interrelated traits, such as curvature, fluidity, lamellarity, and composition[1]. While the role of membrane bilayers in shaping the structure and function of their associated proteins is well studied[2], the biological significance of more subtle membrane characteristics, such as compositional asymmetry and membrane curvature , are burgeoning areas of investigation[3,4]. Elucidating their biochemical roles will require the ability to synthesize increasingly complex membranes[5] that exhibit the full scope of these traits.

Systematic membrane assembly from simple starting materials is a long-standing challenge. Bulk-scale membrane assembly, such as phospholipid film hydration[6], yields no control over vesicle size, content, membrane composition, and lamellarity. These highly heterogeneous preparations nonetheless pervade in vitro studies of membrane biochemistry because they require no specialized equipment and the experimenter can hunt for the right

*Correspondence: briandna@scripps.edu.

Additional Information: The authors declare no competing financial interests.

Author Contributions: B.M.P. and S.M. conceived and designed the experiments, analyzed the resulting data and co-authored the paper. S.M. executed all experimental work.

vesicle to analyze if needed. Microfluidic vesicle assembly dramatically expands the scope and magnitude of control because sample manipulations that are usually irreproducible on the bulk scale, such as emulsification or mixing, are highly reproducible on the microfluidic scale[7-10]. The products of microfluidic assembly are strikingly homogeneous in size (1–5% CV), encapsulate cargo with high efficiency (> 80%), and are strictly unilamellar. Still, the more nuanced parameters of vesicle configuration, such as lipid leaflet compositional asymmetry, are challenging to control[11,12], and programming lamellarity lies beyond the horizon of current synthetic capabilities.

Lamellarity and leaflet asymmetry are closely intertwined from the perspective of membrane construction. Controlling either parameter implies the ability to specify the composition and number of individual lipid monolayers during construction. Pautot *et al.*[13] introduced a deposition-based strategy that achieved such control for bulk unilamellar vesicle assembly starting from lipid-stabilized water-in-oil emulsions. Centrifuging such an emulsion layered above an oil/water interface forces the emulsified water droplets through the phase boundary, depositing an outer lipid leaflet with composition corresponding to the interface-adsorbed lipids. Numerous experimental observations have supported their proposed mechanism, such as asymmetric bilayer production when different lipids stabilize the emulsion and interface[14], membrane protein insertion and function[15], and faithful recapitulation of bilayer assembly after microfluidic dissection into droplet and interface components[16]. Though these experiments suggest that the mechanism is extensible to constructing more complex membranes, the only published examples produce unilamellar structures.

We hypothesize that a series of lipid monolayer depositions is a viable route to membranes of arbitrarily complex composition and lamellarity. Such a layer-by-layer (LbL) approach to vesicle assembly, reminiscent of Langmuir-Blodgett film deposition[17], would proceed on liquid phase droplets with monolayer deposition occurring only when the droplets cross an oil/water phase boundary. Though mobilizing droplets through a stationary phase boundary multiple times is experimentally intractable[18], mobilizing multiple phase boundaries over droplets trapped in a microfluidic droplet array[19] is straightforward (Fig. 1). Starting from trapped water-in-oil droplets (Fig. 1a), each phase boundary crossing deposits a new monolayer of lipids on the immobilized droplets (Fig. 1c, e, g). Maintaining the phase and changing lipid composition (Fig. 1b, f) programs the monolayer composition for the subsequent deposition step. With this conceptual framework in place, we sought to demonstrate LbL membrane assembly of asymmetric unilamellar and multilamellar membranes.

Results and Discussion

We constructed a static droplet array capable of driving multiple phase boundaries over a collection of trapped droplets to test LbL membrane assembly. The device architecture (Fig. 2) contains a flow-focusing droplet generator that produces monodisperse lipid-stabilized water-in-oil droplets[20], a droplet delay line that acts as a fluidic resistor between downstream components and flow-focusing inputs, and a droplet array chamber containing 15 capture cups. Three fluidic inputs deliver reagents to the circuit, one each for oil-lipid

mixture (dioleoylphosphatidylcholine, DOPC, dissolved in squalene), the cytoplasmic aqueous phase that resides in the interior of the assembled vesicles (AQ_{cy}, typically TAE buffer), and extracellular aqueous phase (AQ_{ex}, typically TAE buffer). Flow-focusing AQ_{cy} with oil-lipid phase generates AQ_{cy}-containing lipid-stabilized droplets. The droplets travel through the delay line, which allows adequate time for lipid stabilization[21] to occur and provides a resistor that insulates the array from any upstream manipulations, such as introducing new sample inputs. After traveling through the delay line, the lipid-stabilized droplets arrive at the 15-cup array where each capture cup immobilizes a single droplet. Terminating AQ_{cy} flow while continuing oil-lipid flow through the array chamber purges excess droplets. The first LbL deposition step proceeds as AQ_{ex} flow initiates, driving a phase boundary over the trapped droplets to yield unilamellar vesicles (Movie S1). The product vesicles are visibly different from the droplet starting materials when imaged in differential interference contrast (DIC) mode because the AQ_{cy} and AQ_{ex} refractive indices of vesicles are essentially identical whereas the AQ_{cy} and oil-lipid indices of droplets are quite different. Confocal fluorescence imaging of membrane-labeled vesicles revealed the expected annular sections (Fig. 2).

We first conducted selective permeabilization assays to test whether the vesicle products were unilamellar after a single deposition. These assays measure the activity of hemolysin, a soluble pore-forming protein that spontaneously inserts into and selectively permeabilizes membranes to small molecules and ions[22]. Perfusing hemolysin into an array of symmetric vesicles assembled from DOPC (**1**) and loaded with both fluorescein (332 Da, green fluorescence) and cascade blue dextran (10 kDa, blue fluorescence) size exclusion markers resulted in synchronized loss of green fluorescence and retention of blue fluorescence in multiple vesicles (Fig. 3a). We similarly observed selective permeabilization in vesicles loaded with DNA encoding the hemolysin gene, fluorescent size exclusion markers, and an in vitro transcription/translation system[23], albeit with substantially increased time to onset of fluorescein leakage (Fig. 3b).

These preliminary studies establish LbL membrane assembly as analogous to the conventional assembly mode[13] based on mobilizing droplets through stationary oil/water phase boundaries. Selective permeabilization assays prove that LbL membranes are unilamellar because hemolysin only permeabilizes single bilayers. The assay also demonstrates the biological relevance of these synthetic bilayers in supporting insertion and assembly of a membrane protein pore complex. Loading the vesicles with genetic material and minimal cellular metabolism provides further corroborating evidence that the product bilayers are unilamellar and moreover can serve as compartments and scaffolds for displaying functional membrane-associated proteins. This is a key step toward in vitro evolution of membrane protein function[24] and a systematic analytical approach to single-vesicle scale synthetic biology[25].

Next we tested the extensibility of LbL membrane assembly in the controlled construction of a multilamellar membrane. If the proposed mechanism holds, we should be able to isolate and characterize unilamellar vesicles and triple monolayer water-in-oil droplets, the two predicted intermediates of double bilayer vesicle assembly. Dithionite chemical probing[26] of asymmetric unilamellar vesicles prepared with fluorescent nitrobenzoxadiazole (NBD)

headgroup-labeled DOPC derivative **2** in the outer (L_2) lipid leaflet resulted in fluorescence quenching, however, membrane-impermeable dithionite was unable to quench membrane fluorescence when **2** was deposited in the internal L_1 leaflet (Fig. 4a). Triple monolayer droplet intermediates prepared with fluorescent NBD tail-labeled DOPC derivative **3** in the outer (L_3) leaflet and perfused with Co(II) ethylhexanoate (an oil-soluble collisional quencher) again resulted in fluorescence quenching[27]. Depositing **3** one monolayer away from the external leaflet in L_2 produced intermediates that resisted quenching with Co(II) (Fig. 4b). Dithionite treatment of bilamellar vesicles formed by an additional monolayer deposition of **2** in either the inner (L_3) or the outer (L_4) leaflet rapidly quenched the fluorescence of L_4-labeled vesicles, but not L_3-labeled vesicles (Fig. 4c).

With chemical probing data in hand, we sought to examine overall lamellarity of the structure by quantitating the amount of material deposited in each assembly step. Incorporating fluorescent reporter lipids in not just a single defined monolayer, but rather each monolayer during assembly provides a means for quantitating material deposited over a series of depositions. Layer-by-layer assemblies of double bilayer vesicles constructed with **2** in each of the four constituent lamellae exhibited increasing fluorescence intensity with each monolayer deposition as assembly proceeded. If each leaflet contains approximately the same surface area, fluorescence should increase linearly. Furthermore, selective external leaflet quenching of these multiply-labeled intermediates and final double bilayer product should yield a fraction of the construct total fluorescence that is inversely proportional to the number of depositions[28]. Our observations agree with linear and inverse proportionality for the layer-by-layer construction and selective external leaflet quenching experiments, respectively (Fig. 5).

The chemical probing experiments and quantitation of sequential depositions *in situ* are orthogonal evidence that together establish LbL assembly as a route to phospholipid membranes with defined compositional asymmetry and lamellarity. During the course of multilamellar membrane construction, DIC images of each assembly intermediate exhibit the expected contrast: water-in-oil droplets are strongly contrasted, unilamellar vesicles are weakly contrasted, triple monolayer droplets resemble the starting droplet precursors with strong contrast, and double bilayer vesicles resemble unilamellar intermediates with weak contrast. Chemical probing of the intermediates with membrane-impermeable fluorescence quenchers generated data consistent with highly controlled reporter lipid positioning, with lamellar localization corresponding directly with the order of lipid addition during assembly. Leaflet-specific lipid deposition, the existence of asymmetric unilamellar and triple monolayer droplets, and the quantitative addition of four sequential reporter-containing monolayers substantiate the proposed synthesis and structure of the product double bilayer vesicle.

Droplet trapping and LbL assembly provides a highly systematic approach to membrane bilayer preparation. During droplet loading prior to membrane assembly, droplets flow over the array until a satisfactory percentage of the array is filled. Once a cup is filled, droplet flow diverts around the cup rather than filling it with a second droplet[19]. Droplet trapping occurred at a rate of 12 ± 2 filled capture cups for the array of 15 in this device (n = 15 array loading experiments). Vesicle size is tunable by changing droplet size[16], though constrained

by the array's ability to capture the droplets for deposition. Droplets and vesicles of this study averaged 55 μm diameter, extending the range to 10–100 μm diameter should be possible with cups appropriately redesigned either with smaller drains to capture smaller droplets or larger size and deeper array chamber to accommodate larger droplets. Varying the chemical composition of the oil-lipid phase and the number of depositions programs individual lipid monolayer composition within the product membrane and the overall lamellarity. Low-resolution imaging of multiple vesicles undergoing parallel treatment (quenching, permeabilization) yielded some membrane structures that qualitatively appeared inhomogeneous, an observation we attributed to diffraction-limited optical imaging. While it is possible that parts of the structures are inhomogeneous due to, for example, residual oil trapped in the bilayer during assembly, we neither detect it during quantitative chemical probing or high-resolution DIC imaging nor observe inhibition of membrane protein insertion and function. Nonetheless, we cannot exclude the possibility that some of the structures are inhomogeneous. Even higher resolution electron microscopy-based imaging will be required to verify membrane morphology.

From an experimental perspective, the vesicle arrays generated during LbL membrane assembly also dramatically simplify, systematize and parallelize the synthesis of bilayer membranes and their characterization. Flow and interface conditions are both controlled and easily visualized during assembly. The moving phase boundary driven by positive pressure during layer-by-layer assembly is analogous to centrifugation-mediated mobilization of droplets through a static phase boundary in the experimental approach of Pautot *et al.*[14]. Visualizing the phase boundary crossing during assembly reveals that bilayer assembly can occur under conditions of dramatically varying droplet/phase boundary relative velocities (~0.1 mm/s during layer-by-layer assembly versus 1–10 mm/s during centrifugation). Array immobilization reproducibly positions multiple vesicles in the same field of view, enabling reproducibility studies through parallel quantitative imaging of multiple independent vesicles. For example, obtaining encapsulation efficiency data over multiple vesicles entails imaging the array before and after deposition; encapsulation efficiency of small molecule cargo fluorescein and macromolecular cargo 10 kDa dextran were 91 ± 5% and 95 ± 3%, respectively (Fig. S1), measured over 30 vesicles assembled in 5 experiments and in agreement with previous studies[16]. Further hemolysin treatment of these arrays experiments yielded 30 total replicate selective permeabilization experiments (Fig. S2). Though the array configuration is ideal for prototyping membrane assembly and quantitative imaging, it is not suited to large-scale production. Implementing LbL membrane assembly principles with continuous flow[29] would provide production of material for more sample-intensive structural characterization techniques.

LbL membrane assembly now provides a route to asymmetric unilamellar and double bilayer membranes, complex phospholipid-based cellular structures that were previously difficult or impossible to prepare in the laboratory. Asymmetric LbL membrane assembly can serve as a new tool for studying lipid biosynthesis enzymes and transporters that collectively give rise to and maintain biological membrane asymmetry. Multilamellar LbL membrane assembly provides access to scaffolds that resemble complex cellular membrane systems (e.g. nuclear envelope, mitochondrial membrane). Protein complexes associated

with such membranes that require multilamellar contexts for function in vivo can now be reconstituted and studied in proper synthetic scaffolds. This is particularly important in the case of the nuclear pore complex, where mechanistic studies of pore assembly do not yet have appropriate in vitro model systems[30].

In conclusion, we describe a systematic route to arbitrarily complex phospholipid membranes and an experimental platform that enables straightforward replicate quantitative analysis of membrane protein activity. Unilamellar vesicles support functional insertion and assembly of a pore-forming protein complex and can compartmentalize and support a basic cell-like metabolism. LbL membrane assembly is the first synthetic strategy for accessing compositionally asymmetric multilamellar structures, which are prevalent in all cellular membrane systems.

Methods

Unless otherwise noted, all reagents were delivered to the circuit at 2.1 μL/min and aqueous phase was TAE buffer. Oil-lipid **1** phase was phospholipid **1** (1 mM) and cholesterol (10 mol%) dissolved in squalene. Fluorescent lipid mixtures were prepared with unlabeled phospholipid **1** (1 mM), cholesterol (10 mol%) and either head-labeled phospholipid **2** (1 mol%) or tail-labeled phospholipid **3** (1 mol%) dissolved in squalene. These mixtures are denoted oil-lipid **2** and oil-lipid **3**, respectively.

Droplet trapping and symmetric unilamellar vesicle assembly

Water droplets were generated at a flow focusing intersection. Oil-lipid **1** was driven into the circuit at the oil-lipid input. Aqueous phase (0.2 μl/min) was driven into the circuit at the AQ_{cy} input. Water droplets flowing in oil-lipid **1** were driven to the array of capture cups for droplet trapping. Once the capture cup array was filled, AQ_{cy} flow was terminated and untrapped droplets were purged from the array with additional oil-lipid **1** washing. Finally, the trapped droplet array was flushed with aqueous phase until all oil phase was removed (~10 min, Movie S1). High-resolution images of droplets and vesicles were acquired (60X / 1.42 NA, IX-81 FV1000, Olympus, Center Valley, PA) using oil immersion and devices fabricated on #0 cover glass backing.

Encapsulation yield determination

Aqueous phase containing Cascade Blue-labeled dextran (1% w/w) and fluorescein dye (10 μM) was driven into the circuit at the AQ_{cy} input and formed into droplets. Routine quantitative confocal fluorescence imaging was performed at low magnification (10X / 0.4 NA) using devices fabricated on standard microscope slide backing. Droplet array images were acquired in both the Cascade Blue channel ($\lambda_{ex}/\lambda_{em}$ = 400 nm/420 nm) and fluorescein channel ($\lambda_{ex}/\lambda_{em}$ = 490 nm/520 nm). The trapped droplets were used as templates for LBL vesicle assembly as described. Vesicular cargo fluorescence was measured in the same channels. Image data were quantitated using a circular region of interest (ROI) in ImageJ (Fig. S1, NIH, Bethesda, MD)[31] and vesicular fluorescence divided by droplet fluorescence to arrive at encapsulation yield.

Selective permeabilization assay

Vesicles loaded with Cascade Blue-labeled dextran and fluorescein were prepared as described. The array was perfused with alpha hemolysin (10 μg/ml, TAE) and intravesicular fluorescence monitored. Confocal fluorescence imaging microscopy time courses of both dextran and fluorescein fluorescence were acquired , and intensity data quantitated using ROIs that include the vesicle contents (Fig. S3).

Asymmetric unilamellar vesicle assembly

Asymmetric vesicles with fluorescently labeled inner leaflet L_1 were prepared by generating aqueous droplets in head-labeled oil-lipid **2**. Captured droplets were washed with unlabeled oil-lipid **1** before flushing with aqueous phase. Vesicles with fluorescently labeled outer leaflet L_2 were prepared by generating aqueous droplets in oil-lipid **1**. Captured droplets were washed with oil-lipid **2** before conversion into vesicles by flushing with aqueous phase. Both inner- and outer-labeled vesicle arrays were perfused with aqueous $S_2O_4^{2-}$ (50 mM), imaged at low magnification (20X / 0.75, $\lambda_{ex}/\lambda_{em}$ = 490 nm/520 nm) and fluorescence data quantitated as before using ROIs that include the entire membrane (Fig. S4).

Triple monolayer droplet assembly

An array of aqueous droplets in oil-lipid **1** was prepared as a starting scaffold (see above). Triple monolayer droplets with fluorescently labeled interior leaflet L_2 were prepared by flushing the trapped droplet array with tail-labeled oil-lipid **3**, followed by aqueous phase and then oil-lipid **1**. Triple monolayer droplets with fluorescently labeled oil-exposed monolayer L_3 were prepared by first flushing the trapped droplet array with oil-lipid **1**, followed by aqueous phase and then oil-lipid **3**. Finally, oil-lipid **3** was replaced with unlabeled oil-lipid **1** for imaging. Both L_2- and L_3-labeled triple monolayer droplet arrays were perfused with cobalt(II) 2-ethylhexanoate in mineral oil (0.13% wt/wt) and NBD reporter fluorescence quantitated as in the asymmetric vesicle assembly experiment above (Fig. S5).

Double bilayer vesicle assembly

Symmetric unilamellar vesicles were assembled as starting scaffolds (see above). Double bilayer vesicles with fluorescently labeled leaflet L_3 were prepared by flushing the unilamellar vesicle array with head-labeled oil-lipid **2**, followed by unlabeled oil-lipid **1**, then aqueous phase. Double bilayer vesicles with fluorescently labeled leaflet L_4 were prepared by flushing the unilamellar vesicle array with oil-lipid **1**, followed by oil-lipid **2**, then aqueous phase. Both L_3- and L_4-labeled double bilayer vesicles were perfused with $S_2O_4^{2-}$ and NBD reporter fluorescence quantitated as in the asymmetric vesicle assembly experiment above (Fig. S6).

Quantitation of LbL deposition

Double bilayer vesicles were assembled with all leaflets (L_1–L_4) fluorescently labelled with **2**. Symmetric unilamellar vesicles were first prepared by generating aqueous droplets in oil-lipid **2** to image L_1 fluorescence, followed by aqueous phase to image L_1+L_2 fluorescence. The array was next flushed with oil-lipid **2** to image L_1+L_2+L_3 fluorescence, and finally

aqueous phase to image L_1+L_2+L_3+L_4 fluorescence. Confocal fluorescence images were analyzed as before. Total fluorescence counts for each assembly intermediate were divided by the fluorescence of the final double bilayer product to yield the normalized to the total membrane fluorescence of 4 monolayers. The external lipid monolayer fluorescence of water-in-oil droplet and triple-monolayer droplet intermediates was selectively quenched by 40-min perfusion with cobalt(II) 2-ethylhexanoate. The external lipid monolayer fluorescence of unilamellar and double bilayer vesicles was selectively quenched by 40-min perfusion with dithionite. The membrane fluorescence of the quenched constructs was divided by that of the pre-quenched construct to yield the fraction of the membrane-resident molecules remaining fluorescent and therefore protected from the external quenching agent.

Supplementary Material

Refer to Web version on PubMed Central for supplementary material.

Acknowledgments

This work was supported by an NIH Pathway to Independence Career Development Award (GM083155) and a NSF CAREER Award (1255250) to B.M.P.

References

1. van Meer G, Voelker DR, Feigenson GW. Membrane lipids: where they are and how they behave. Nat Rev Mol Cell Bio. 2008; 9:112–124. [PubMed: 18216768]
2. Rosenbaum DM, Rasmussen SGF, Kobilka BK. The structure and function of G-protein-coupled receptors. Nature. 2009; 459:356–363. [PubMed: 19458711]
3. Peter B, et al. BAR domains as sensors of membrane curvature: The amphiphysin BAR structure. Science. 2004; 303:495–499. [PubMed: 14645856]
4. Hatzakis NS, et al. How curved membranes recruit amphipathic helices and protein anchoring motifs. Nat Chem Biol. 2009; 5:835–841. [PubMed: 19749743]
5. Liu AP, Fletcher DA. Biology under construction: in vitro reconstitution of cellular function. Nat Rev Mol Cell Bio. 2009; 10:644–650. [PubMed: 19672276]
6. Bangham AD, Standish MM, Watkins JC. Diffusion of univalent ions across lamellae of swollen phospholipids. J Mol Biol. 1965; 13:238–&. [PubMed: 5859039]
7. Jahn A, Vreeland WN, Gaitan M, Locascio LE. Controlled vesicle self-assembly in microfluidic channels with hydrodynamic focusing. J Am Chem Soc. 2004; 126:2674–2675. [PubMed: 14995164]
8. Shum HC, Lee D, Yoon I, Kodger T, Weitz DA. Double emulsion templated monodisperse phospholipid vesicles. Langmuir. 2008; 24:7651–7653. [PubMed: 18613709]
9. Stachowiak JC, et al. Unilamellar vesicle formation and encapsulation by microfluidic jetting. Proc Natl Acad Sci U S A. 2008; 105:4697–4702. [PubMed: 18353990]
10. Ota S, Yoshizawa S, Takeuchi S. Microfluidic formation of monodisperse, cell-sized, and unilamellar vesicles. Angew Chem Int Edit. 2009; 48:6533–6537.
11. Richmond DL, et al. Forming giant vesicles with controlled membrane composition, asymmetry, and contents. Proc Natl Acad Sci U S A. 2011; 108:9431–9436. [PubMed: 21593410]
12. Hu PC, Li S, Malmstadt N. Microfluidic fabrication of asymmetric giant lipid vesicles. ACS Appl Mater Interfaces. 2011; 3:1434–1440. [PubMed: 21449588]
13. Pautot S, Frisken BJ, Weitz DA. Production of unilamellar vesicles using an inverted emulsion. Langmuir. 2003; 19:2870–2879.
14. Pautot S, Frisken B, Weitz D. Engineering asymmetric vesicles. Proc Natl Acad Sci U S A. 2003; 100:10718–10721. [PubMed: 12963816]

15. Noireaux V, Libchaber A. A vesicle bioreactor as a step toward an artificial cell assembly. Proc Natl Acad Sci U S A. 2004; 101:17669–17674. [PubMed: 15591347]
16. Matosevic S, Paegel BM. Stepwise synthesis of giant unilamellar vesicles on a microfluidic assembly line. J Am Chem Soc. 2011; 133:2798–2800. [PubMed: 21309555]
17. Blodgett K. Films built by depositing successive monomolecular layers on a solid surface. J Am Chem Soc. 1935; 57:1007–1022.
18. Hase M, Yamada A, Hamada T, Yoshikawa K. Transport of a cell-sized phospholipid micro-container across water/oil interface. Chem Phys Lett. 2006; 426:441–444.
19. Huebner A, et al. Static microdroplet arrays: a microfluidic device for droplet trapping, incubation and release for enzymatic and cell-based assays. Lab Chip. 2009; 9:692–698. [PubMed: 19224019]
20. Anna S, Bontoux N, Stone H. Formation of dispersions using ‘flow focusing’ in microchannels. Appl Phys Lett. 2003; 82:364–366.
21. Baret JC, Kleinschmidt F, Harrak A El, Griffiths AD. Kinetic aspects of emulsion stabilization by surfactants: a microfluidic analysis. Langmuir. 2009; 25:6088–6093. [PubMed: 19292501]
22. Song L, et al. Structure of staphylococcal alpha-hemolysin, a heptameric transmembrane pore. Science. 1996; 274:1859–1866. [PubMed: 8943190]
23. Shimizu Y, et al. Cell-free translation reconstituted with purified components. Nat Biotechnol. 2001; 19:751–755. [PubMed: 11479568]
24. Tawfik DS, Griffiths A. Man-made cell-like compartments for molecular evolution. Nat Biotechnol. 1998; 16:652–656. [PubMed: 9661199]
25. Andes-Koback M, Keating CD. Complete budding and asymmetric division of primitive model cells to produce daughter vesicles with different interior and membrane compositions. J Am Chem Soc. 2011; 133:9545–9555. [PubMed: 21591721]
26. McIntyre JC, Sleight RG. Fluorescence assay for phospholipid membrane asymmetry. Biochemistry. 1991; 30:11819–11827. [PubMed: 1751498]
27. Morris SJ, Bradley D, Blumenthal R. The use of cobalt ions as a collisional quencher to probe surface charge and stability of fluorescently labeled bilayer vesicles. Biochim Biophys Acta. 1985; 818:365–372. [PubMed: 4041444]
28. Heider EC, Barhoum M, Edwards K, Gericke KH, Harris JM. Structural characterization of individual vesicles using fluorescence microscopy. Anal Chem. 2011; 83:4909–4915. [PubMed: 21574603]
29. Kantak C, Beyer S, Yobas L, Bansal T, Trau D. A ‘microfluidic pinball’ for on-chip generation of layer-by-layer polyelectrolyte microcapsules. Lab Chip. 2011; 11:1030–1035. [PubMed: 21218225]
30. Antonin W, Ellenberg J, Dultz E. Nuclear pore complex assembly through the cell cycle: Regulation and membrane organization. FEBS Lett. 2008; 582:2004–2016. [PubMed: 18328825]
31. Schneider CA, Rasband WS, Eliceiri KW. NIH Image to ImageJ: 25 years of image analysis. Nat Chem Biol. 2012; 9:671–675.

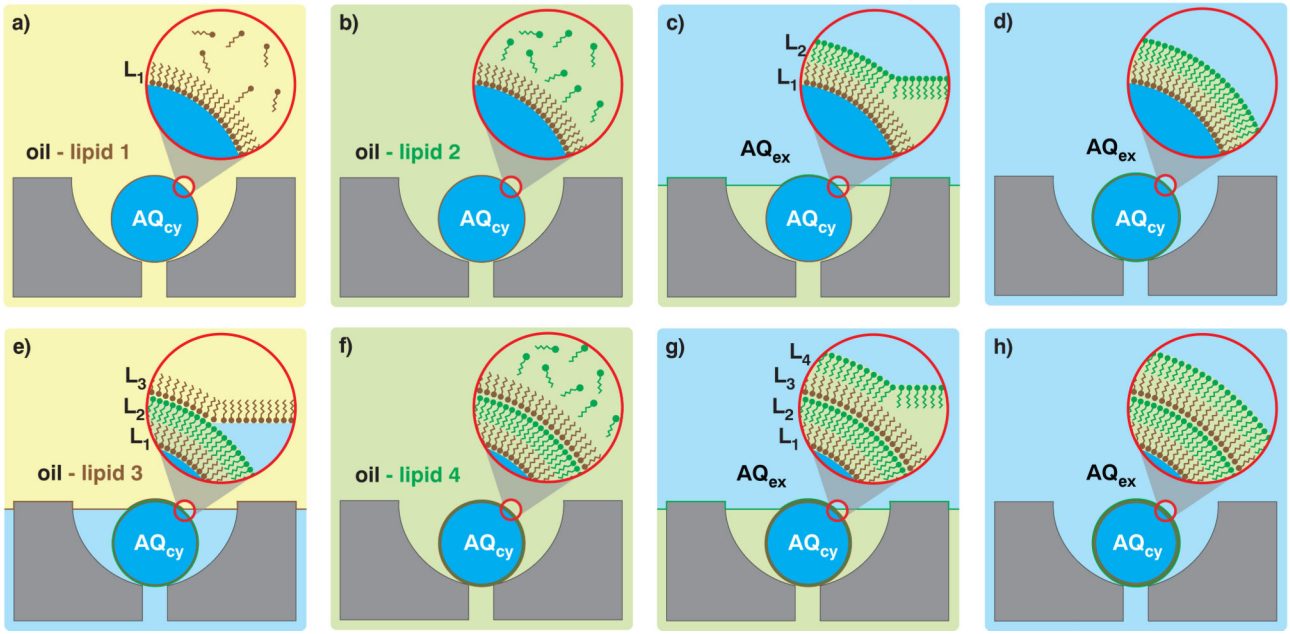

Figure 1. Layer-by-layer assembly schematic

a, Capture cups each retain a single droplet that contains aqueous cytoplasmic material (AQ_{cy}, *blue*) in a mixture of oil-lipid 1 (*yellow*). A monolayer of lipid 1 stabilizes the droplets. **b,** Oil-lipid 2 (*green*) mixture replaces oil-lipid 1. **c,** Extracellular aqueous phase (AQ_{ex}, *blue*) replaces oil-lipid 2. As the AQ_{ex}/oil interface traverses the array, it envelopes each trapped droplet and lipids in the interfacial monolayer composed of oil-lipid 2 deposit on the trapped droplets. **d,** Complete exterior phase exchange transforms the droplets into unilamellar vesicles. **e,** Exchanging AQ_{ex} with oil-lipid 3 deposits a third lipid leaflet onto the unilamellar vesicle to produce a triple monolayer droplet. **f–g,** Introducing oil-lipid 4 followed by AQ_{ex} deposits a final fourth leaflet of lipids. **h,** The final product after three phase exchanges is a double bilayer vesicle.

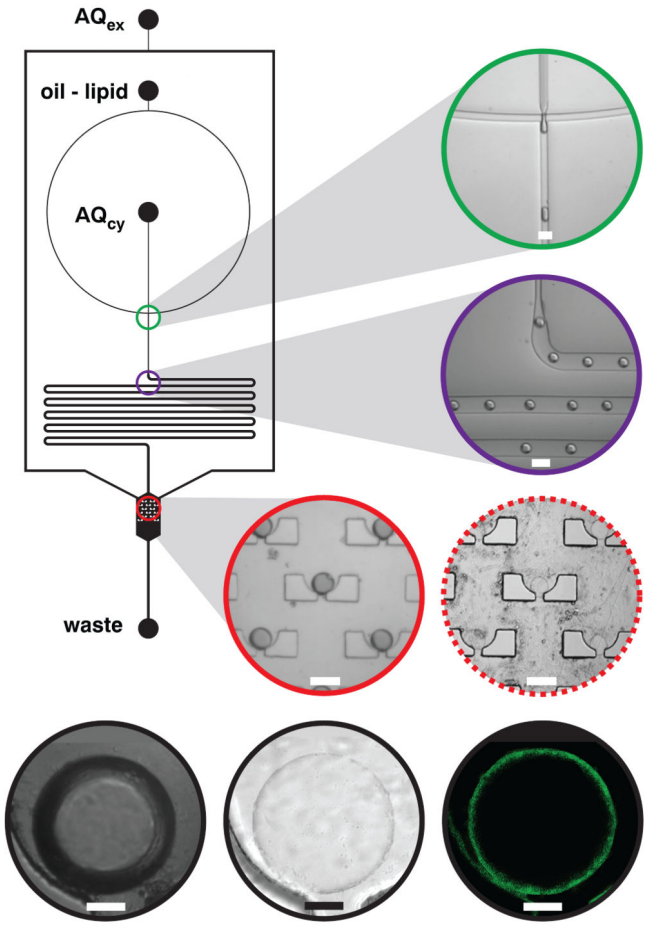

Figure 2. Vesicle assembly circuit schematic and imaging

Three fluidic inputs deliver extracellular aqueous medium (AQ_{ex},TAE buffer), oil-lipid mixture (DOPC in squalene, CMC = 2 mM), and cytoplasmic aqueous medium (AQ_{cy},TAE buffer) to the circuit and one output removes fluids to waste. The capture array chamber is 1.2 mm wide. Each 120-μm-diameter cup contains a 30-μm-wide drain. All other channels are 120 μm wide. Channel depth is 50 μm. DOPC-stabilized water-in-oil droplets emerge from the flow-focusing junction (*green*, scale = 100 μm), travel through a delay line (*violet*, scale = 100 μm) and arrive at the droplet capture chamber (*red*, scale = 100 μm) where an array of cups captures single droplets. Driving a phase boundary over the trapped droplets deposits an external monolayer of lipids, transforming the water-in-oil droplets into vesicles (*dashed red*, scale = 100 μm). High-resolution DIC imaging of a trapped droplet displays strong DIC between the internal aqueous and external oil phase (*black left*, scale = 20 μm), but after a single monolayer deposition, the refractive indices of the external and internal aqueous phase contrast weakly (*black center*, scale = 20 μm). High-resolution confocal fluorescence imaging of the same vesicle labeled with fluorescent lipid **2** yielded clean annular sections (*black right*, scale = 20 μm).

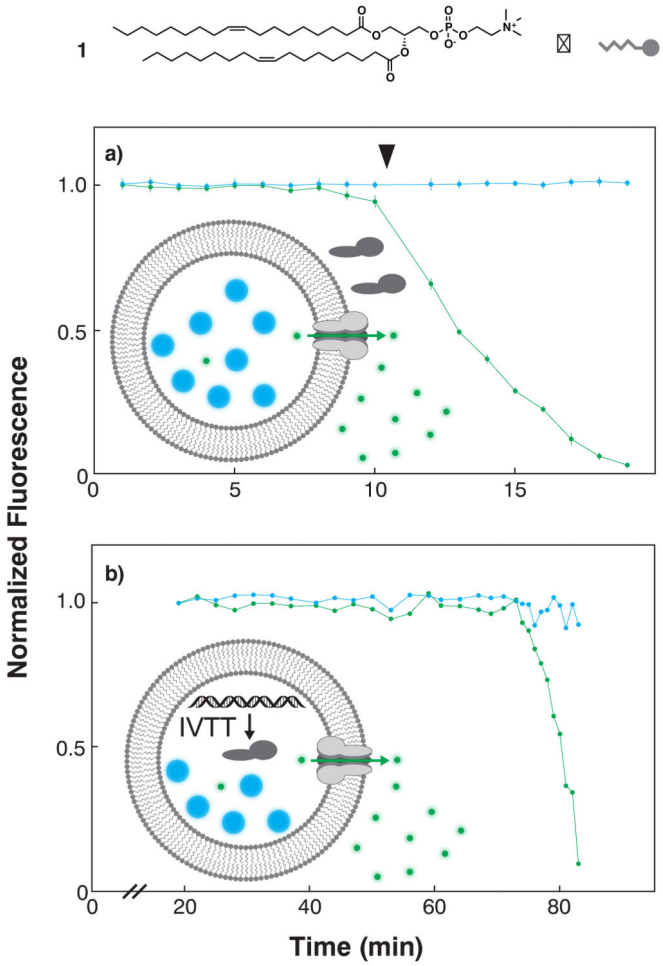

Figure 3. Membrane protein synthesis and function in LbL vesicles

a, Symmetric vesicles were assembled with DOPC (**1**), loaded with fluorescein/10-kDa dextran size exclusion markers, perfused with purified hemolysin and intravesicular fluorescence monitored for multiple vesicles (n=7). Time-dependent loss of fluorescein fluorescence (*green*) and invariance in dextran fluorescence (*blue*) signified selective membrane permeabilization toward fluorescein, confirming that the product membrane is unilamellar and that the membrane protein is functionally reconstituted. **b,** Vesicles loaded with DNA encoding the hemolysin gene, RNA transcription components, protein translation components, and fluorescein/10-kDa dextran size exclusion markers were incubated to allow in vitro transcription/translation (IVTT) of hemolysin monomers, membrane incorporation of monomers, pore complex assembly and function. Pore function was followed as in **a.**

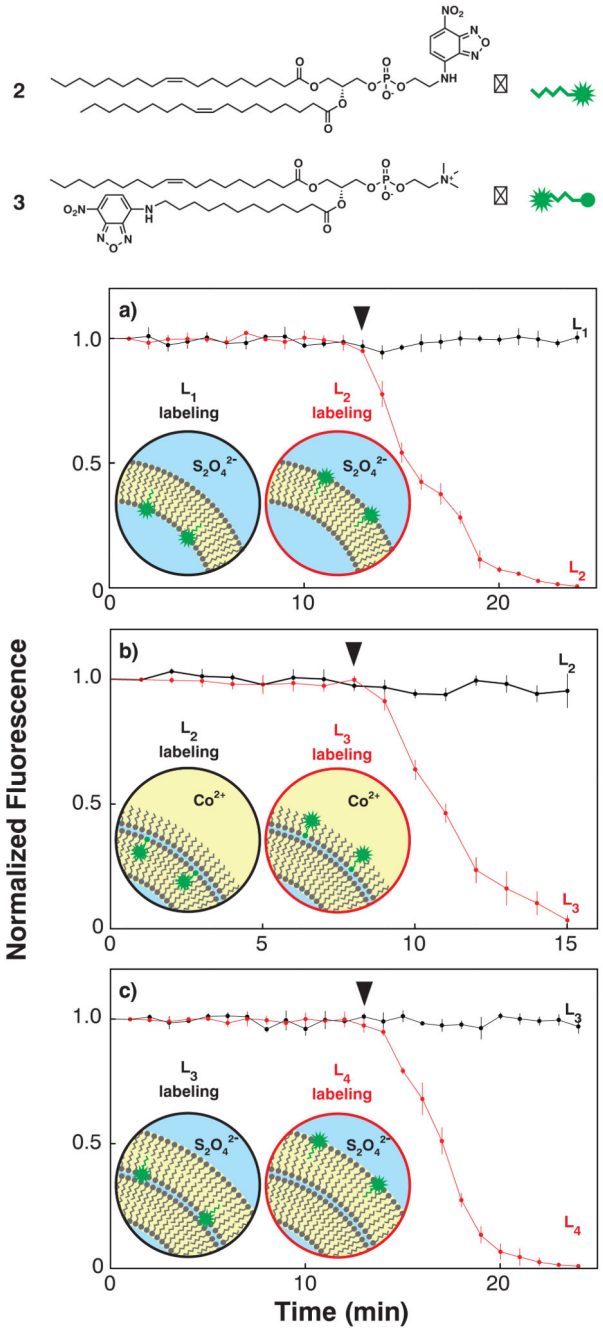

Figure 4. Double bilayer assembly intermediate and final product chemical probing

Fluorescent reporter lipids used for chemical probing included N-NBD-labeled dioleolylphosphatidylethanolamine (**2**) and 12-NBD-dodecyl-labeled oleoylphosphatidylcholine (**3**). Stars (✹) indicate the position of the NBD fluorophore within the reporter lipid structures. **a,** Treating unilamellar vesicles assembled with **2** in either the cytoplasmic L_1 leaflet (*black*) or the extracellular L_2 leaflet (*red*) with membrane-impermeable reductive quenching agent $S_2O_4^{2-}$ (▼) selectively quenches the membrane fluorescence of L_2-labeled vesicles (n = 3). **b,** Treating triple monolayer water-in-oil droplets assembled with **3** in either the internal leaflet L_2 (*black*) or the oil-exposed leaflet

L_3 (*red*) with the oil-soluble collisional quenching agent Co(II) (▼) selectively quenches the membrane fluorescence of L_3-labeled vesicles (n = 3). **c,** Treating double bilayer vesicles assembled with **2** in either the penultimate leaflet L_3 (*black*) or the extracellular leaflet L_4 (*red*) with $S_2O_4^{2-}$ (▼) selectively quenches the membrane fluorescence of L_4-labeled vesicles (n = 3). Insets schematize the proposed assembly intermediates and products, leaflet localization of reporter lipids, and location of NBD fluorophore.

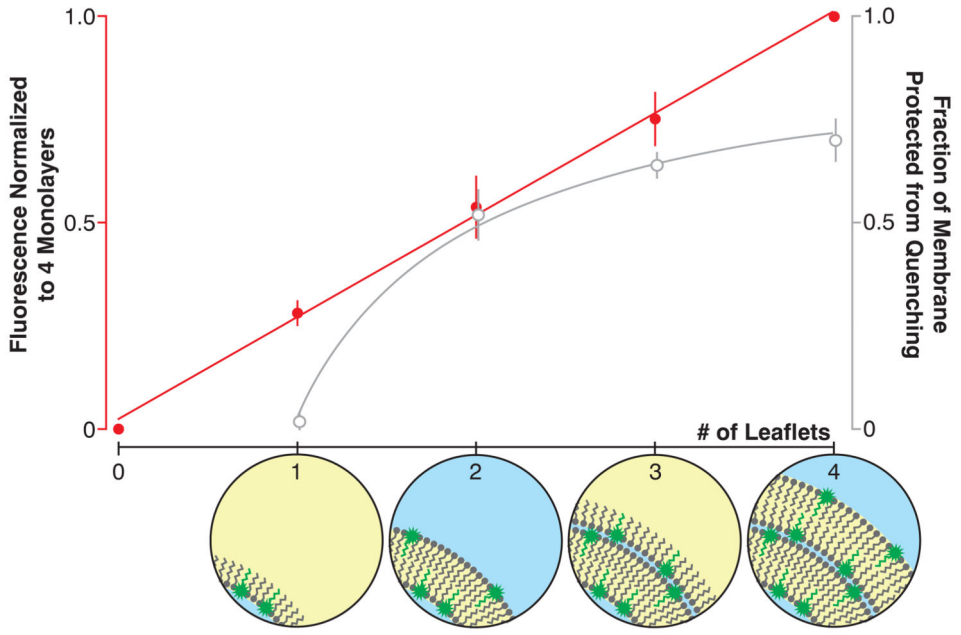

Figure 5. Quantitative layer-by-layer deposition

Layer-by-layer deposition of lipid monolayers containing 1 mol% **2** yielded vesicles with membrane fluorescence that varied in agreement with predicted models of deposition-dependent fluorescence. Membrane fluorescence normalized to the intensity of structures generated after 3 monolayer depositions (4 putative monolayers) and plotted as a function of the number of depositions increases linearly (left axis, red circles and trend line; slope = 0.247 ± .007, R^2 = 0.998, 5 experiments). Membrane fluorescence after quenching the external leaflet and normalizing to the intensity of the unquenched construct increases asymptotically, proportional to the inverse of the number of depositions (right axis, open gray circles and trend line, X intercept = 0.97 ± .05, R^2 = 0.995, 6 experiments). *X axis insets* schematize the LbL assembly intermediates en route to a double bilayer membrane with equimolar **2** in each monolayer.